

RBF Approximation of the Lippmann-Schwinger Equation

Nadaniela Egidi, Josephin Giacomini and Pierluigi Maponi

School of Science and Technology, University of Camerino, Camerino, Italy

Article history

Received: 03-03-2023

Revised: 08-04-2023

Accepted: 13-04-2023

Corresponding Author:

Josephin Giacomini

School of Science and
Technology University of

Camerino, Camerino, Italy

Email: josephin.giacomini@unicam.it

Abstract: We consider the direct scattering problem that consists of the computation of the scattered wave generated by an incident plane wave and an inhomogeneous object defined in terms of the refractive index. From some suitable physical and geometrical hypotheses, this is formulated as a boundary value problem for the Helmholtz equation and, in turn, as the Lippmann-Schwinger equation. For the numerical solution of this integral equation, we propose an approximation approach by using Radial Basis Functions (RBF), which allows a relevant reduction in the computational cost of the numerical procedure. This new method is described in full detail and its performance is shown by using a wide numerical experiment for the approximate solution of the Lippmann-Schwinger equation with different approaches.

Keywords: Lippmann-Schwinger Equation, RBF Approximation, Direct Scattering

Introduction

Scattering is a general term used to describe several physical phenomena where moving particles or radiation, such as light or sound, interact with obstacles in the medium through which they pass. It involves several physical processes, such as for example acoustic scattering (Adam, 2017), electromagnetic scattering (Mansuripur, 2020), elastic scattering (Saleem, 2015), and quantum scattering (Belkic, 2020), and gives the conceptual basis and practical tools to study and solve several remote sensing problems in engineering (Wade and Drake, 2019), medicine and biology (Charalambopoulos *et al.*, 2008) and geology (Mao *et al.*, 2021) just to give some examples. So, the analysis of scattering problems has a relevant role in the theoretical and applied scientific literature, see (Ramm, 2017; Osipov and Tretyakov, 2017; Devaney, 2012) for nice surveys in this field.

The scattering problems are usually distinguished from direct scattering problems, providing the mathematical formulation to define and compute the scattered field from the knowledge of the scatterer and the incident field and inverse scattering problems, which define the mathematical procedures to compute some properties of the scatterer from the knowledge of the scattered fields generated by known incident fields. These two problems have quite different natures; the direct problem is usually well-posed and consists of the solution of a boundary-value problem for one or several differential equations. On the other hand, the inverse problem is ill-posed and its usual formulation is based on

one or several integral equations. However, these two classes of scattering problems are actually strictly connected since almost all solution procedures for inverse scattering problems require the solution of the corresponding direct scattering problem, (van den Berg and Kleinman, 1997; Egidi and Maponi, 2010; 2011) for some examples on this connection between direct and inverse problems. This connection has given importance to the direct problems and their numerical solution as a fundamental tool in the reconstruction procedures.

The numerical solution of the direct scattering problems has been studied in a large number of scientific papers and different numerical approaches have been proposed, such as for example (Elschner and Hu, 2012; Dong *et al.*, 2022) propose a Galerkin method for the approximate solutions of the integral formulation of direct scattering problems; (Coifman *et al.*, 1999; Maponi, 2005; Egidi *et al.*, 2007; Egidi and Maponi, 2008; 2004) propose perturbation approaches for the integral formulation of the direct scattering problem; (Ganesh and Hawkinsb, 2019; Egidi and Maponi, 2009) propose a fast multipole method for the integral formulation of the direct scattering problem; (Kanaun, 2015) proposes a Gaussian-RBF method to numerically solve the integral formulation of a direct scattering problem; (Li *et al.*, 2018) the numerical solution of the differential form of the problem equipped with perfectly matched layer; (Duhamel, 2022) the finite element solution of the differential form of the problem; (Li *et al.*, 2018) the numerical solution of the differential form of the problem equipped with absorbing boundary conditions.

In this study, we consider a time-harmonic electromagnetic scattering problem, where the symmetries of the obstacle and of the incident wave allow the formulation of the problem by a boundary value problem for the Helmholtz equation. For this problem, a simple application of the green formulas gives rise to the Lippmann-Schwinger equation, which is an integral equation appearing in several scattering problems in acoustics (Prunty and Snieder, 2020), electromagnetism (Kirsch and Lechleiter, 2009) and quantum mechanics (Kukulin and Rubtsova, 2003). So, any advance in the solution of this equation constitutes a relevant contribution to the theoretical and applied analysis of scattering problems. We propose an RBF approach to the numerical solution of the Lippmann-Schwinger equation based on the collocation method (Atta and Youssri, 2022; Youssri and Atta, 2023). The proposed method allows a reduced computational cost of the approximation scheme when a suitable decomposition is used for the elements in the considered radial basis, see (Egidi, 2022) for details. However, this method can be easily generalized to other RBF kernels and other integral equations. We provide a detailed description of this method and a wide numerical experiment to test its numerical performance.

The Formulation of the Scattering Problem

We start by introducing the main notation. Let \mathbb{R}, \mathbb{C} be the set of real numbers and complex numbers, respectively. Let $\mathbb{R}^N, \mathbb{C}^N$ be the N -dimensional real Euclidean space and the N -dimensional complex Euclidean space, respectively. Let $\underline{x}, \underline{y} \in \mathbb{R}^N$, we denote with $\underline{x}^t \underline{y}$ the Euclidean scalar product of \underline{x} and \underline{y} , the superscript t means transposed and $\|\underline{x}\|$ denotes the Euclidean norm of \underline{x} . Let $\mathbb{S} = \{\underline{x} \in \mathbb{R}^2: \|\underline{x}\| = 1\}$. We denote i the imaginary unit. We denote with $\mathbb{R}^{M \times N}, \mathbb{C}^{M \times N}$ the space of real and complex matrices, respectively, having M rows and N columns.

We consider an electromagnetic wave propagating in a homogeneous medium containing a penetrable obstacle. The interaction of the wave with the obstacle generates a scattered electromagnetic wave. We consider the following direct scattering problem: compute the scattered electromagnetic field from the knowledge of the obstacle and the incident electromagnetic field.

In the aforementioned problem, we assume that the obstacle is completely characterized by the refractive index. Moreover, some physical and geometrical assumptions are considered in order to simplify the formulation of the problem: (a) the obstacle has cylindrical symmetry and, for simplicity, its symmetry axis coincides with a coordinate axis, (b) The obstacle

cross section is bounded, (c) All the electromagnetic waves are time-harmonic with wave number $k > 0$, (d) the incident electromagnetic wave is an electromagnetic plane wave having polarization parallel to the symmetry axis of the obstacle. These assumptions allow the reduction of the Maxwell equations. In particular, let u be the component of the electric field parallel to the polarization vector, and let $\underline{x} = (x_1, x_2)' \in \mathbb{R}^2$ be the variables along the coordinate plane orthogonal to the symmetry axis of the obstacle. From the symmetry of the problem, we have that u depends only from \underline{x} and, by straightforward calculation with the Maxwell equations, it is the solution to the problem ((Stratton, 2007) Chapter 6 and (Maponi *et al.*, 1997)):

$$\Delta u + k^2 n(\underline{x})u = 0, \underline{x} \in \mathbb{R}^2 \tag{1}$$

$$u(\underline{x}) = u^i(\underline{x}) + u^s(\underline{x}), \underline{x} \in \mathbb{R}^2 \tag{2}$$

$$\lim_{\|\underline{x}\| \rightarrow +\infty} \sqrt{\|\underline{x}\|} (\hat{\underline{x}}^t \cdot \nabla u^s - iku^s) = 0, \hat{\underline{x}} \in \mathbb{S} \tag{3}$$

where, Δ is the Laplacian operator, ∇ is the gradient operator, k is the wave number, $n(\underline{x})$ is the refractive index of the medium at $\underline{x} \in \mathbb{R}^2$, $u^i(\underline{x}) = e^{ik\underline{d}^t \underline{x}}$, $\underline{x} \in \mathbb{R}^2$ is the incident plane wave with direction $\underline{d} = (\cos \alpha, \sin \alpha)'$, $u^s(\underline{x})$, $\underline{x} \in \mathbb{R}^2$ is the scattered wave, $\hat{\underline{x}} = \frac{\underline{x}}{\|\underline{x}\|} \in \mathbb{S}$, $\underline{x} \neq \underline{0}$. We note that (3) is the Sommerfeld radiation condition and gives a boundary condition for the problem (1-3). The solution to this problem is the scattered wave u^s and it can be used in a more precise definition of the direct scattering problem: Given k, \underline{a}, n ; compute the solution $u^s(\underline{x})$, $\underline{x} \in \mathbb{R}^2$, of the problem (1-3). Let L be the characteristic size of the obstacle, we consider the wave number k in the resonance region, that is $kL|n| \approx 1$, where other approximations like high/low-frequency expansions are not possible.

We also suppose that the refractive index $n = 1$ outside the obstacle, so the contrast index $m(\underline{x}) = 1 - n(\underline{x})$, $\underline{x} \in \mathbb{R}^2$ has a support set coinciding with the position $D \subset \mathbb{R}^2$ of the scatterer. From hypothesis (b) above, we have that D is a bounded set; let $B \subset \mathbb{R}^2$ be a domain such that $B \supseteq D$, from the problem (1-3) and the Green formulas we can obtain the Lippmann-Schwinger equation (Colton and Kress, 2019):

$$u(\underline{x}) + \frac{ik^2}{4} \int_B H_0^{(1)}(k\|\underline{x} - \underline{y}\|) m(\underline{y}) u(\underline{y}) d\underline{y} = u^i(\underline{x}), \underline{x} \in B \supseteq D \tag{4}$$

where, $H_0^{(1)}$ is the Hankel function of first kind and order 0, (Abramowitz and Stegun, 1965) for details. For integral Eq. (4) there exist several results of the existence and uniqueness of the solution, (Colton and Kress, 2019) for the case of bounded inhomogeneities.

Remark (circular inhomogeneity). We consider a circular inhomogeneity:

$$n(\underline{x}) = \begin{cases} n_0, & \|\underline{x}\| < R \\ 1, & \|\underline{x}\| > R \end{cases} \quad (5)$$

where, $n_0 \in \mathbb{C}$, $n_0 \neq 1$, is a constant refractive index and $R > 0$ gives the radius of the obstacle. In this case, the solution of Eq. (4) can be expressed as follows:

$$u(\underline{x}) = \begin{cases} \sum_{l=-\infty}^{\infty} \frac{2l^{l-1}}{\pi k R D_l} J_l(k\sqrt{n_0}\|\underline{x}\|) e^{ik(\theta_x - \alpha)}, & \|\underline{x}\| < R \\ u^i(\underline{x}) - \sum_{l=-\infty}^{\infty} l \frac{N_l}{D_l} H_l^{(1)}(k\|\underline{x}\|) e^{ik(\theta_x - \alpha)}, & \|\underline{x}\| > R \end{cases} \quad (6)$$

where, $\theta_x \in [0, 2\pi)$ is the angular variable of \underline{x} , J_l is the Bessel function of order l and H_l is the Hankel function of the first kind and order l , (Abramowitz and Stegun, 1965) for details; moreover:

$$D_l = H_{l+1}^{(1)}(kR) J_l(k\sqrt{n_0}R) - \sqrt{n_0} H_l^{(1)}(kR) J_{l+1}(k\sqrt{n_0}R)$$

$$N_l = J_{l+1}(kR) J_l(k\sqrt{n_0}R) - \sqrt{n_0} J_l(kR) J_{l+1}(k\sqrt{n_0}R)$$

Appendix A gives a schematic proof of this formula.

The Numerical Solution of the Lippmann-Schwinger Equation

We consider the collocation method for the numerical solution of Eq. (4). So, the approximation U of u is given by:

$$U(\underline{x}) = \sum_{i=1}^L c_i \phi_i(\underline{x}), \underline{x} \in B \quad (7)$$

where, $\{\phi_1, \phi_2, \dots, \phi_L\}$ are known independent functions and $\{c_1, c_2, \dots, c_L\}$ are unknown coefficients. Given L distinct points $\underline{x}_1, \underline{x}_2, \dots, \underline{x}_L \in B$, usually called collocation nodes, we consider:

$$\sum_{i=1}^L \left(\phi_i(\underline{x}_j) + \frac{ik^2}{4} \int_B H_0^{(1)}(k\|\underline{x}_j - \underline{y}\|) m(\underline{y}) \phi_i(\underline{y}) d\underline{y} \right) c_i = u^i(\underline{x}_j), j = 1, 2, \dots, L \quad (8)$$

which is a linear system for the coefficients $\{c_1, c_2, \dots, c_L\}$. Each entry of the coefficient matrix requires the computation of a two-dimensional integral of a non-smooth function, in fact, the Hankel function $H_0^{(1)}$ has an integrable singularity at the origin and the contrast index m is usually characterized by bounded jumps. We note that quadrature formulas can be easily adapted to the continuity properties of m in the solution of the direct scattering problems since function m is known, but this is a hard task in the solution of the inverse problem where (4) has to be solved with different tentative functions m without precise information on its continuity properties.

As a consequence, the computational time of matrix entries in (8) is a critical aspect of the numerical solution of this linear system.

A possible approach to reduce the computational time of matrix entries in (8) is given by the approximation of the integral operator in (4) through degenerate integral operators. These operators have an integral kernel expressed as a sum of terms made of two factors: one depending on variable \underline{x} , the other depending on the variable \underline{y} , (Kress, 1999) for details; so, these kernels resemble the addition formula for Hankel functions, see formula (17) in the appendix. Unfortunately, this formula has no global convergence and cannot be easily used in (8).

We propose to approximate the integral operator in (4) by a new family of degenerate integral operators defined through the use of a radial basis in (7). More precisely, let $\underline{y}_1, \underline{y}_2, \dots, \underline{y}_L \in B$ be given points, we define:

$$\phi_l(\underline{x}) = \Phi(\|\underline{x} - \underline{y}_l\|), \underline{x} \in B, l = 1, 2, \dots, L \quad (9)$$

So, linear system (8) becomes:

$$\sum_{i=1}^L (\Phi(\|\underline{x}_j - \underline{x}_i\|) + \frac{ik^2}{4} \int_B H_0^{(1)}(k\|\underline{x}_j - \underline{y}\|) m(\underline{y}) \Phi(\|\underline{y} - \underline{x}_i\|) d\underline{y}) c_i = u^i(\underline{x}_j), j = 1, 2, \dots, L \quad (10)$$

where, we have used collocation nodes as *RBF* centers, i.e., $\underline{y}_l = \underline{x}_l, l = 1, 2, \dots, L$. We can observe that in (10) function Φ plays a similar role to the integral kernel $H_0^{(1)}$. This can be profitably used in the definition of degenerate integral operators that approximate the original operator; in fact, the integral kernel is a datum of the problem instead function Φ can be chosen as one of many possible RBF kernels (Fasshauer, 2007). We show this approximation procedure for a particular choice of a mother function Φ , i.e., the inverse multiquadric function, but this approach can be easily generalized to other RBF kernels and also other integral equations.

Thus, we consider the inverse multiquadric function with shape parameter τ :

$$\Phi(\|\underline{x} - \underline{y}\|) = \frac{1}{\sqrt{\tau^2 + \|\underline{x} - \underline{y}\|^2}} = \frac{1}{\|\underline{X} - \underline{Y}\|} \quad (11)$$

where, $\underline{X} = (\underline{x}^t, 0)^t, \underline{Y} = (\underline{y}^t, \tau)^t \in \mathbb{R}^3$, with $\underline{x}, \underline{y} \in \mathbb{R}^2$.

Let $(\rho_x, \pi/2, \omega_x), \rho_x \geq 0, \omega_x \in [0, 2\pi)$ be the spherical coordinates of $\underline{X}, (t_y, \varphi_y, \omega_y), t_y = \sqrt{\tau^2 + \|\underline{y}\|^2}, \varphi_y \in [0, \pi], \omega_y \in [0, 2\pi)$ be the spherical coordinates of \underline{Y} . From Taylor expansion of (11) at $\rho_x = 0$ we can show that (Egidi, 2022):

$$\Phi(\|\underline{x} - \underline{y}\|) = \sum_{n=0}^{\infty} \sum_{v=0}^n \mathcal{E}_v \frac{(n-v)!}{(n+v)!} P_n^v(0) P_n^v(\cos \varphi_y) \cos(m(\omega_y - \omega_x)) \frac{\rho_x^n}{t_y^{n+1}} = \sum_{n=0}^{\infty} \sum_{v=0}^{2n} \mathcal{G}_{n,v}(\underline{x}) f_{n,v}(\underline{y}) \quad (12)$$

where $\varepsilon_\nu = 1$ if $\nu = 0$ and $\varepsilon_\nu = 2$ if $\nu > 0$, for $\nu = 0, 1, \dots, n$, P_n^ν are the Legendre functions of degree n and order ν , (Abramowitz and Stegun, 1965) for details. We note that, in each addendum of the series in (12), functions $g_{n,\nu}, f_{n,\nu}$, $\nu = 0, 1, \dots, 2n, n \in \mathbb{N}$ gather all the terms depending on \underline{x} , \underline{y} respectively; in particular, each index $\nu > 0$ in the first expression generates two addenda in the second expression due to the addition formula for cosine.

The convergence of the series in (12) is guaranteed for $\rho_x < \rho_y$; however, its rate of convergence is a critical aspect in devising an effective approximation of the integral kernel in (4). To this aim, we can improve the convergence rate of this series by a translation argument; in particular, let $\underline{z} \in \mathbb{R}^2$ be a point near \underline{x} such that $\|\underline{x} - \underline{z}\| \ll \|\underline{z} - \underline{y}\|$, then formula (4) can be considered for function:

$$\Phi(\|\underline{x} - \underline{y}\|) = \Phi(\|(\underline{x} - \underline{z}) - (\underline{y} - \underline{z})\|) = \Phi(\|\underline{\zeta} - \underline{\eta}\|) \quad (13)$$

where, the new variables $\underline{\zeta} = \underline{x} - \underline{z}$, $\underline{\eta} = \underline{y} - \underline{z}$ ensure a higher convergence rate for series in (4).

We note that translation techniques are at the base of fast multipole methods (Ganesh and Hawkinsb, 2019; Egidi and Maponi, 2009), however, the following numerical example shows the efficacy of the expansion (12) enhanced with the translation (13) in our case.

Example (Decomposition of the inverse multiquadric function by using the translation). We consider function (11) with $\underline{x}, \underline{y} \in [0,1] \times [0,1]$. Table 1 reports the maximum absolute error E in formula (12), where the series is truncated at $n = d$. The error E is computed by using $N = 1024$ points in a uniform Cartesian grid of $[0,1] \times [0,1]$; moreover, the translation variables \underline{z} are given by $N_z = 16$ points in a uniform Cartesian grid of $[0,1] \times [0,1]$. The error E_0 is computed in the same way but without using the translation strategy, i.e., $\underline{z} = \underline{0}$ is considered.

We consider the decomposition formula (12) to approximate the entries of the coefficient matrix in (10). Let $\{B_1, B_2, \dots, B_S\}$ be a partition of B and $\underline{z}_s \in B_s$, $s = 1, 2, \dots, S$ be proper translation variables. Let $d \in \mathbb{N}$ be the truncation index in the series of formulas (12). We denote with $A_{j,l}$, $j, l = 1, 2, \dots, L$ the entries of the coefficient matrix in (10); from (12) and (13) we have the following approximation:

$$\begin{aligned} A_{j,l} &= \Phi(\|\underline{x}_j - \underline{x}_l\|) + \frac{ik^2}{4} \int_B H_0^{(1)}(k\|\underline{x}_j - \underline{y}\|) m(\underline{y}) \Phi(\|\underline{y} - \underline{x}_l\|) d\underline{y} = \\ & \Phi(\|\underline{x}_j - \underline{x}_l\|) + \frac{ik^2}{4} \sum_{s=1}^S \int_{B_s} H_0^{(1)}(k\|\underline{x}_j - \underline{y}\|) m(\underline{y}) \Phi(\|\underline{y} - \underline{x}_l\|) d\underline{y} \approx \\ & \Phi(\|\underline{x}_j - \underline{x}_l\|) + \frac{ik^2}{4} \sum_{s=1}^S \sum_{n=0}^{2n} \left(\int_{B_s} H_0^{(1)}(k\|\underline{x}_j - \underline{y}\|) m(\underline{y}) f_{n,\nu}(\underline{y} - \underline{z}_s) d\underline{y} \right) \\ & g_{n,\nu}(\underline{x}_j - \underline{z}_s) \end{aligned} \quad (14)$$

Table 1: Error in the decomposition formula (12) with the translation (13)

τ	d	E	E_0
1	8	$1.15 \cdot 10^{-8}$	2.57
1	10	$2.56 \cdot 10^{-10}$	4.61
10	8	$6.93 \cdot 10^{-17}$	$4.34 \cdot 10^{-10}$
10	10	$6.98 \cdot 10^{-17}$	$8.04 \cdot 10^{-12}$
0.5	8	$9.95 \cdot 10^{-7}$	$1.36 \cdot 10^3$
0.5	10	$09.95 \cdot 10^{-7}$	$3.77 \cdot 10^3$

Hence, the approximation of the coefficient matrix A has the following structure:

$$A \approx \Phi + FG \quad (15)$$

where, $\Phi \in \mathbb{R}^{L \times L}$ as entries given by the first addendum on the right-hand side of (14), $F \in \mathbb{R}^{L \times S(d+1)^2}$ has entries given by the integral terms and $G \in \mathbb{R}^{S(d+1)^2 \times L}$ has entries given by functions $g_{n,\nu}$, $\nu = 0, 1, \dots, 2n, n \in \mathbb{N}$ and different translation variables. So, if we suppose that all functions in formula (15) have negligible cost with respect to the costs C_B , and C_S of the numerical integration over B , B_s , respectively, for the computational costs $C_A, C_{\Phi+FG}$ of the coefficient matrix in (10) and (14), respectively, we have:

$$C_A = L^2 C_B$$

$$C_{\Phi+FG} = S(d+1)^2 LC_B$$

Moreover, if we suppose $C_S = C_B/S$, since B is partitioned in $\{B_1, B_2, \dots, B_S\}$, we obtain:

$$C_{\Phi+FG} = (d+1)^2 LC_B$$

So, the decomposition of matrix A allows a reduction of the computational cost of (10) when $(d+1)^2 < L$. We note that also matrix Φ can be decomposed by (12), however, this is usually not convenient from a computational point of view.

Results

We present the results of a numerical experiment to test the performance of the proposed method. In the numerical test, we consider the solution of the Lippman-Schwinger Eq. (4), or equivalently the boundary value problem (1-3), for obstacles having different shapes and different refractive indices, these obstacles are described in (Fig. 1).

So, we consider the four obstacles obtained by combining these shapes, i.e., Circle (center $\underline{0}$ and radius 1), Square (center $\underline{0}$ and edge length 2), and these refractive indices, i.e., n_1 and n_2 . For all the obstacles, Eq. (4) is defined by using $B = [-1.5, 1.5] \times [-1.5, 1.5]$. A unique wave number, i.e., $k = 1$, and a unique incidence direction, i.e., $\alpha = \frac{\pi}{3}$ are considered for the sake of brevity, however, analogous results can be obtained for wave numbers with similar magnitude and different incident waves.

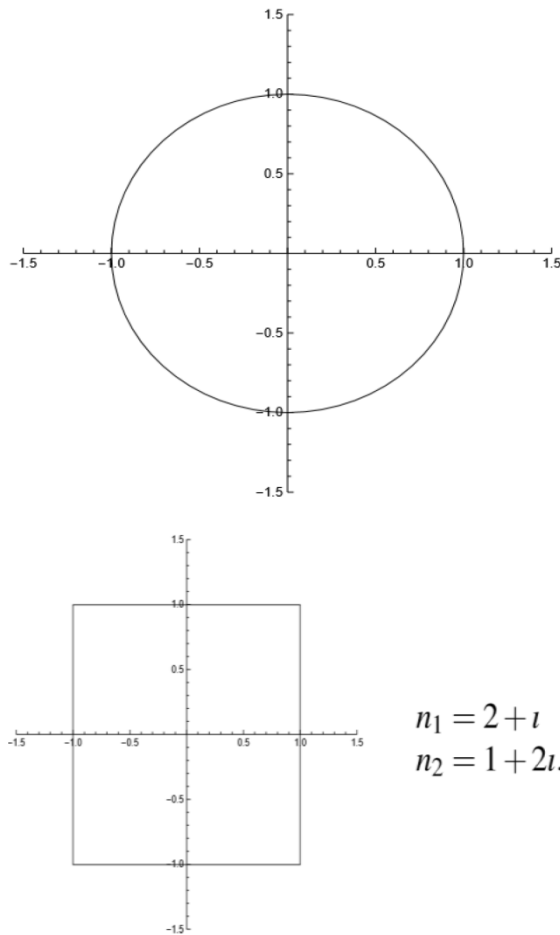


Fig. 1: The obstacles considered in the numerical experiment (from top to bottom): Circle, square and the refractive indices on the right

The numerical solution of (4) is computed by using the discretization scheme (8) with different representation bases:

- RBF** The base (11) is used in (8), so the discretization scheme (10) is solved to compute the coefficients $\{c_1, c_2, \dots, c_L\}$ of (7)
- DEC** The base (11) is used in (8) together with the decomposition (12), so the coefficients $\{c_1, c_2, \dots, c_L\}$ of (7) are computed by the discretization scheme (10) with the approximated coefficient matrix (14), where $\{B_1, B_2, \dots, B_S\}$ is a uniform partition of B and \underline{z}_s the center of B_s , $s = 1, 2, \dots, S$
- PWB** Let $G = \{(a_p, b_q) \in B, \text{ with } a_0 < a_1 < \dots < a_p, b_0 < b_1 < \dots < b_Q, P, Q \in \mathbb{N}\}$, be a grid on B . In (7), we consider the piecewise bilinear base on this grid, so for each index l in (7) there exists $(a_p, b_q) \in G$ such that $\phi_l(a_p, b_q) = 1$, $\phi_l(\underline{x}) = 0$, $\underline{x} \in [a_{p-1}, a_{p+1}] \times [b_{q-1}, b_{q+1}]$ and ϕ_l is a bilinear function in each interval $[a_{i-1}, a_i] \times [b_{j-1}, b_j]$ with $i = p$,

$p+1, j = q, q+1$. This base is used in (8), which is solved to compute the coefficients $\{c_1, c_2, \dots, c_L\}$ of (7). In particular, the numerical experiment is done with uniform grids G on B

In Tables 2-3 and (Fig. 2) the different methods are compared in terms of the accuracy and the computational cost of the numerical solution of (4). The accuracy is evaluated by the relative l^2 error E in the numerical solution of (4); the parameter E is computed by using formula (6), which gives the exact solution in the case of circular obstacles and by using the approximation method itself with a finer discretization in the case of square obstacles. In particular, the parameter E in Table 2 (circular obstacles) is computed by formula (6), where the series index is truncated to $|l| = 20$. In Table 3 (square obstacles) the parameter E_{PWB} for the PWB method with $L = N^2$ basis elements is computed by the same method with $L = (N+1)^2$ basis elements. The parameters E_{RBF} , and E_{DEC} for RBF and DEC methods, respectively, with $L = N^2$ RBF elements are computed by the RBF method with $L = (N+1)^2$ RBF elements. It is worth noting that the shape parameter τ in methods RBF and DEC has been calibrated by using circular obstacles, where the exact solution is known. The computational cost is evaluated by the elapsed time T (in seconds) in the numerical solution of (4). Integrals in (8), (10), and (14) are evaluated by a generalized Gauss-Legendre quadrature formula. The solution of linear systems (8), (10) is computed by Gaussian elimination with partial pivoting.

From Tables (2-3) and (Fig. 2) we can see that the collocation method gives satisfactory results with all the considered bases. In particular, RBF has a higher computational cost than PWB, but it gives also more accurate numerical solutions of (4). It is worth noting that the DEC method provides a more accurate result than the PWB method and with a reduced computational cost with respect to the RBF method when the two parameters S and d have been properly chosen. A preliminary rule arising from these results is to prefer the increase of parameter S with respect to the increase of d . However, a proper balance of these two parameters with respect to the particular problem to be solved is probably the right rule to obtain the best performance of the DEC method. Future studies of this method have to establish such a rule to select optimal parameters S and d .

All the results have been obtained by Matlab software package running on a workstation HP EliteDesk 800G3 TWR, equipped with Intel(R) Core(TM) i7-7700 CPU 3.60GHz, with 32GB RAM and operative system Microsoft Windows 10 Pro.

Table 2: Numerical results for the two obstacles with shape Circles. For every method: L is the number of base elements in (7), this column is shared by all the methods; E is the relative l^2 error in the numerical solution of (4); T is the elapsed time (in seconds) in the numerical solution of (4); τ is the shape parameter in (11), this column is shared by methods RBF and DEC; S and d are the decomposition parameters in (14) (only method DEC). The notation $x(y)$ stays for $x \cdot 10^y$

Shape: Circle-refractive index: n_1									
L	PWB		τ	RBF		DEC			
	E_{PWB}	T_{PWB}		E_{RBF}	T_{RBF}	S	d	E_{DEC}	T_{DEC}
25	5.9(-2)	2.4(-1)	2.5	1.5(-2)	2.9(0)	25	5	2.4(-2)	2.9(0)
25			2.5			100	5	1.5(-2)	1.1(1)
25			2.5			100	10	1.5(-2)	3.5(1)
100	1.2(-2)	4.0(0)	1.0	2.8(-3)	4.2(1)	25	5	1.9(-2)	1.1(1)
100			1.0			100	5	5.4(-3)	4.1(1)
100			1.0			100	10	5.4(-3)	1.3(2)
400	2.8(-3)	6.3(1)	1.0	1.3(-3)	6.9(2)	25	5	4.0(-2)	4.2(1)
400			1.0			100	5	4.4(-3)	1.7(2)
400			1.0			100	10	4.6(-3)	5.5(2)
Shape: Circle-refractive index: n_2									
25	5.3(-2)	2.1(-1)	2.5	1.8(-2)	2.9(0)	25	5	2.9(-2)	2.7(0)
25			2.5			100	5	1.8(-2)	1.1(1)
25			2.5			100	10	1.5(-2)	3.5(1)
100	1.1(-2)	3.7(0)	1.0	3.4(-3)	4.2(1)	25	5	2.3(-2)	1.0(1)
100			1.0			100	5	5.6(-3)	4.1(1)
100			1.0			100	10	5.6(-3)	1.3(2)
400	2.9(-3)	6.1(1)	1.0	1.5(-3)	6.4(2)	25	5	4.7(-2)	4.0(1)
400			1.0			100	5	4.7(-3)	1.6(2)
400			1.0			100	10	4.7(-3)	5.3(2)

Table 3: Numerical results for the two obstacles with the shape Square. For every method: L is the number of base elements in (7), this column is shared by all the methods; E is the relative l^2 error in the numerical solution of (4); T is the elapsed time (in seconds) in the numerical solution of (4); τ is the shape parameter in (11), this column is shared by methods RBF and DEC; S and d are the decomposition parameters in (14) (only method DEC). The notation $x(y)$ stays for $x \cdot 10^y$

Shape: Square-refractive index: n_1									
L	PWB		τ	RBF		DEC			
	E_{PWB}	T_{PWB}		E_{RBF}	T_{RBF}	S	d	E_{DEC}	T_{DEC}
25	3.8(-2)	2.4(-1)	2.5	8.2(-3)	2.7(0)	25	5	8.2(-3)	3.0(0)
25			2.5			100	5	7.6(-3)	1.1(1)
25			2.5			100	10	7.6(-3)	3.6(1)
100	7.2(-3)	3.8(0)	1.0	1.5(-3)	4.0(1)	25	5	3.1(-3)	1.1(1)
100			1.0			100	5	5.4(-3)	4.3(1)
100			1.0			100	10	5.4(-3)	1.4(2)
400	1.9(-3)	6.2(1)	1.0	7.6(-4)	6.4(2)	25	5	2.9(-3)	4.3(1)
400			1.0			100	5	3.7(-3)	1.7(2)
400			1.0			100	10	3.7(-3)	5.5(2)
Shape: Square-refractive index: n_2									
25	3.2(-2)	2.1(-1)	2.5	9.5(-3)	2.6(0)	25	5	9.6(-3)	2.8(0)
25			2.5			100	5	8.8(-3)	1.1(1)
25			2.5			100	10	8.8(-3)	3.6(1)
100	7.1(-3)	3.7(0)	1.0	1.7(-3)	4.0(1)	25	5	3.5(-3)	1.1(1)
100			1.0			100	5	4.5(-3)	4.3(1)
100			1.0			100	10	4.5(-3)	1.4(2)
400	1.7(-3)	6.2(1)	1.0	9.1(-4)	6.2(2)	25	5	2.8(-3)	4.3(1)
400			1.0			100	5	3.9(-3)	1.7(2)
400			1.0			100	10	3.9(-3)	5.5(2)

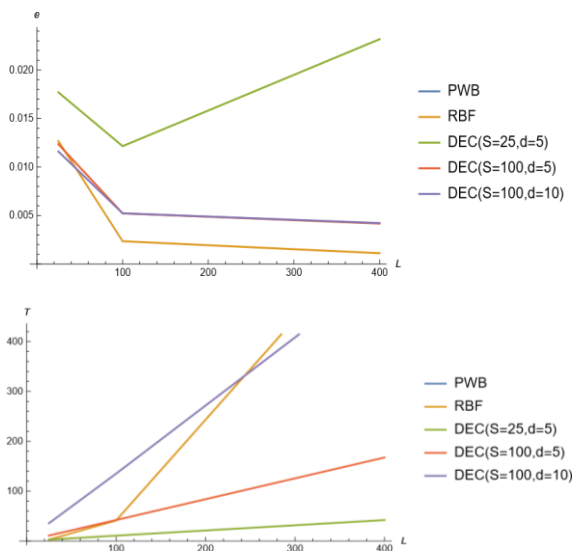


Fig. 2: The results of the numerical experiment (from top to bottom): the average of the errors obtained for the various obstacles (top diagram), the average of the computational time for the various obstacles (bottom diagram)

Conclusion

We considered a direct scattering problem for time-harmonic electromagnetic waves. From some symmetry hypotheses, this problem can be formulated as a two-dimensional boundary value problem for the Helmholtz equation. Moreover, from standard arguments on potential theory, the scattering problem is reformulated as the Lippman-Schwinger equation.

For the solution of this integral equation, we have considered the collocation method with RBF as a representation basis. The resulting discretization scheme has a coefficient matrix defined by two-dimensional integrals for non-smooth integrand functions. So, a critical aspect of this method is the computational cost of the coefficient matrix. In order to overcome this difficulty, we have proposed a decomposition scheme in the special case of inverse multiquadric RBF.

We reported the results of a numerical experiment to test the proposed method. From these results, we can conclude that the RBF-collocation method is able to compute an accurate numerical solution of the Lippmann-Schwinger equation even if the basis is not adapted to the shape of the obstacle; it is worth noting that this is an important feature of the method in the solution of the inverse problem, where the shape of the obstacle is not known. Moreover, the numerical results have shown that the decomposition schemes for RBF can provide a powerful tool to reduce the computational cost of the overall numerical procedure ensuring at the same time a reasonable accuracy in the computed solution.

These promising results deserve further analysis mainly in the stabilization techniques of the approximation scheme, in the improvement of the efficiency of the decomposition by

using the properties of the Hankel function, and in the application of these new discretization schemes in the numerical solution of the inverse scattering problem. To this aim, an important step is the achievement of accurate error estimation in formula (15) in order to have precise control of the translation technique and the expansion formula.

Acknowledgment

Thank you to the publisher for their support in the publication of this research article. We are grateful for the resources and platform provided by the publisher, which have enabled us to share our findings with a wider audience. We appreciate the efforts of the editorial team in reviewing and editing our work, and we are thankful for the opportunity to contribute to the field of research through this publication.

Funding Information

This research received partial funding from Unione Europea-FSE, through Ministero dell'Università e della Ricerca within the call for the project Pon Ricerca e Innovazione 2014-2020 in Decreto Ministeriale 1062-10/08/2021.

Author's Contributions

Nadaniela Egidi and Josephin Giacomini: Methodology, software, written reviewed and edited.

Pierluigi Maponi: Conceptualization, methodology, software, validation, written originally drafted preparation, written reviewed and edited.

All authors have read and agreed to the published version of the manuscript.

Ethics

No ethical issues can arise after the publication of this study.

References

- Abramowitz, M., & Stegun, I. A. (1965). Handbook of Mathematical Functions with Formulas, Graphs, and Mathematical. *New York*, 361.
- Adam, J. A. (2017). *Rays, Waves and Scattering: Topics in Classical Mathematical Physics* (Vol. 56). Princeton University Press.
<https://www.jstor.org/stable/j.ctt1vxm7wt>
- Atta, A. G., & Youssri, Y. H. (2022). Advanced shifted first-kind Chebyshev collocation approach for solving the nonlinear time-fractional partial integro-differential equation with a weakly singular kernel. *Computational and Applied Mathematics*, 41(8), 381.
<https://doi.org/10.1007/s40314-022-02096-7>

- Belkic, D. (2020). *Principles of quantum scattering theory*. CRC Press. ISBN: 10-1420033646.
- Charalambopoulos, A., Fotiadis, D. I., & Polyzos, D. (Eds.). (2008). *Advanced Topics in Scattering and Biomedical Engineering: Proceedings of the Eighth International Workshop on Mathematical Methods in Scattering Theory and Biomedical Engineering*. World Scientific. ISBN: 10-9812814841.
- Coifman, R., Goldberg, M., Hrycak, T., Israeli, M., & Rokhlin, V. (1999). An improved operator expansion algorithm for direct and inverse scattering computations. *Waves in Random Media*, 9(3), 441. <https://doi.org/10.1088/0959-7174/9/3/311>
- Colton, D. L., & Kress, R. (2019). *Inverse acoustic and electromagnetic scattering theory*. Berlin: Springer. <https://doi.org/10.1007/978-3-030-30351-8>
- Devaney, A. J. (2012). *Mathematical foundations of imaging, tomography and wavefield inversion*. Cambridge University Press. ISBN: 10-052111974X.
- Dong, H., Lai, J., & Li, P. (2022). A spectral boundary integral method for the elastic obstacle scattering problem in three dimensions. *Journal of Computational Physics*, 469, 111546. <https://doi.org/10.1016/j.jcp.2022.111546>
- Duhamel, D. (2022). A scaled wave finite element method for computing scalar wave radiation and scattering in exterior domains. *Computer Methods in Applied Mechanics and Engineering*, 392, 114676. <https://doi.org/10.1016/j.cma.2022.114676>
- Egidi, N. (2022). Taylor expansion for RBFS decomposition. AIP Publishing, USA. *To appear in Proceedings of the International Conference on Numerical Analysis and Applied Mathematics*.
- Egidi, N., Gobbi, R., & Maponi, P. (2007). The efficient solution of electromagnetic scattering for inhomogeneous media. *Journal of Computational and Applied Mathematics*, 210(1-2), 175-182. <https://doi.org/10.1016/j.cam.2006.10.061>
- Egidi, N., & Maponi, P. (2004). A perturbative method for direct scattering problems. *Rendiconti di Matematica e delle sue Applicazioni, Roma, Serie VII*, 24(2): 303-320. [https://www1.mat.uniroma1.it/ricerca/rendiconti/ARCHIVIO/2004\(2\)/303-320.pdf](https://www1.mat.uniroma1.it/ricerca/rendiconti/ARCHIVIO/2004(2)/303-320.pdf)
- Egidi, N., & Maponi, P. (2008). Preconditioning techniques for the iterative solution of scattering problems. *Journal of Computational and Applied Mathematics*, 218(2), 229-237. <https://doi.org/10.1016/j.cam.2006.12.023>
- Egidi, N., & Maponi, P. (2009). The efficient solution of direct medium problems by using translation techniques. *Mathematics and Computers in Simulation*, 79(8), 2361-2372. <https://doi.org/10.1016/j.matcom.2009.01.010>
- Egidi, N., & Maponi, P. (2010). An efficient method for the solution of the inverse scattering problem for penetrable obstacles. *Mathematics and Computers in Simulation*, 81(3), 731-741. <https://doi.org/10.1016/j.matcom.2010.09.014>
- Egidi, N., & Maponi, P. (2011). Residual correction techniques for the efficient solution of inverse scattering problems. *Mathematics and Computers in Simulation*, 82(1), 192-204. <https://doi.org/10.1016/j.matcom.2011.01.009>
- Elschner, J., & Hu, G. (2012). Direct and inverse elastic scattering problems for diffraction gratings. *Direct and Inverse Problems in Wave Propagation and Applications*, 101. <https://doi.org/10.1515/9783110282283>
- Fasshauer, G. E. (2007). *Meshfree approximation methods with MATLAB* (Vol. 6). World Scientific. ISBN: 10-981270633X.
- Ganesh, M., & Hawkins, S. C. (2019). A fast high order algorithm for multiple scattering from large sound-hard three-dimensional configurations. *Journal of Computational and Applied Mathematics*, 362, 324-340. <https://doi.org/10.1016/j.cam.2018.10.053>
- Kanaun, S. (2015). Scattering of acoustic waves on a planar screen of arbitrary shape: Direct and inverse problems. *International Journal of Engineering Science*, 92, 28-46. <https://doi.org/10.1016/j.ijengsci.2015.03.004>
- Kirsch, A., & Lechleiter, A. (2009). The operator equations of Lippmann-Schwinger type for acoustic and electromagnetic scattering problems in \mathbb{R}^2 . *Applicable Analysis*, 88(6), 807-830. <https://doi.org/10.1080/00036810903042125>
- Kress, R., (1999). Singular integral equations. *Linear Integral Equations*, 94-124. <https://doi.org/10.1007/978-1-4612-0559-3>
- Kukulin, V. I., & Rubtsova, O. G. A. (2003). Discrete quantum scattering theory. *Theoretical and Mathematical Physics*, 134, 404-426. <https://doi.org/10.1023/A:1022657607306>
- Li, Y., Feng, L., & Zhang, L. (2018). The PML method to solve a class of potential scattering problem with tapered wave incidence. *Journal of Mathematical Analysis and Applications*, 459(2), 1160-1171. <https://doi.org/10.1016/j.jmaa.2017.11.027>
- Mansuripur, M. (2020). A tutorial on the classical theories of electromagnetic scattering and diffraction. *Nanophotonics*, 10(1), 315-342. <https://doi.org/10.1515/nanoph-2020-0348>
- Mao, W., Li, W. & Ouyang, W. (2021). Review of seismic inverse scattering migration and inversion. *Reviews of Geophysics and Planetary Physics*, 52(1): 27-44. <https://doi.org/10.19975/j.dqyxx.2020-008>
- Maponi, P. (2005). A numerical method for a direct obstacle scattering problem. *Applied Numerical Mathematics*, 55(3), 322-333. <https://doi.org/10.1016/j.apnum.2005.04.034>

Maponi, P., Misici, L., & Zirilli, F. (1997). A numerical method to solve the inverse medium problem: An application to the Ipswich data. *IEEE Antennas and Propagation Magazine*, 39(2), 14-19.
<https://doi.org/10.1109/74.584493>

Osipov, A. V., & Tretyakov, S. A. (2017). *Modern electromagnetic scattering theory with applications*. John Wiley & Sons. ISBN: 10-0470512385.

Prunty, A. C., & Snieder, R. K. (2020). An acoustic Lippmann-Schwinger inversion method: Applications and comparison with the linear sampling method. *Journal of Physics Communications*, 4(1), 015007.
<https://doi.org/10.1088/2399-6528/ab6570>

Ramm, A. G. (2017). *Scattering by obstacles and potentials*. World Scientific.
https://www.researchgate.net/publication/323413384_Scattering_by_obstacles_and_potentials

Saleem, M. (2015). Quantum Mechanics. IOP Publishing, Bristol. <https://doi.org/10.1088/978-0-7503-1206-6>

Stratton, J. A. (2007). *Electromagnetic theory* (Vol. 33). John Wiley & Sons. ISBN: 10-0470131535.

Van Den Berg, P. M., & Kleinman, R. E. (1997). A contrast source inversion method. *Inverse Problems*, 13(6), 1607. <https://doi.org/10.1088/0266-5611/13/6/013>

Wade, D. M., & Drake, D. J. (2019). A brief review of modern uses of scattering techniques. *Georgia Journal of Science*, 77(2), 7.
<https://digitalcommons.gaacademy.org/gjs/vol77/iss2/7>

Yousri, Y. H., & Atta, A. G. (2023). Spectral collocation approach via normalized shifted Jacobi polynomials for the nonlinear Lane-Emden equation with fractal-fractional derivative. *Fractal and Fractional*, 7(2), 133. <https://doi.org/10.3390/fractalfract7020133>

Appendix A

The Scattered Field of the Circular Inhomogeneity

We consider the circular inhomogeneity (5). From the separation of variables of the Helmholtz operator in polar coordinates, the solution u of Eq. (4) can be assumed in the following form:

$$u(\underline{x}) = \begin{cases} \sum_{l=-\infty}^{\infty} a_l J_l(k\sqrt{n_0}\|\underline{x}\|)e^{il\theta_x}, & \|\underline{x}\| < R \\ u^i(\underline{x}) + \sum_{l=-\infty}^{\infty} b_l H_l^{(1)}(k\|\underline{x}\|)e^{il\theta_x}, & \|\underline{x}\| > R \end{cases} \quad (16)$$

where, for every integer l , a_l, b_l are unknown coefficients, J_l is the Bessel function of order l and $H_l^{(1)}$ is the Hankel function of first kind and order l , (Abramowitz and Stegun, 1965) for details. We noate that u defined in (16) satisfies the Sommerfeld radiation condition (3) as a consequence of the properties of Hankel functions. The

unknown coefficients in (16) can be computed by substituting this expression in Eq. (4). In this computation, we have to use the addition formula for the Hankel functions and the plane wave expansion, see (Abramowitz and Stegun, 1965) for details:

$$H_0^{(1)}(k\|\underline{x}-\underline{y}\|) = \sum_{l=-\infty}^{\infty} H_l^{(1)}(k\rho_x)J_l(k\rho_y)e^{il(\theta_x-\theta_y)}, \|\underline{x}\| > \|\underline{y}\| \quad (17)$$

$$u^i(\underline{x}) = e^{ik\hat{d}\cdot\underline{x}} = \sum_{l=-\infty}^{\infty} t^l J_l(k\rho_x) e^{il(\theta_x-\alpha)} \quad (18)$$

where, $\hat{d} = (\cos\alpha, \sin\alpha)^t$, $(\rho_x, \theta_x), (\rho_y, \theta_y)$ are the polar coordinates of \underline{x} and \underline{y} , respectively. We note that (17) holds also in the case $\|\underline{x}\| < \|\underline{y}\|$ by exchanging the roles of variables \underline{x} and \underline{y} . We start by considering the integral in (4) for $\underline{x} \in \mathbb{R}^2$, with $\|\underline{x}\| < R$; rewriting this integral in the polar coordinates (ρ_y, θ_y) and substituting (16), (17) we obtain:

$$\begin{aligned} \frac{ik^2}{4} \int_B H_0^{(1)}(k\|\underline{x}-\underline{y}\|) m(\underline{y}) u(\underline{y}) d\underline{y} = \\ \frac{ik^2}{4} \sum_{l,j=-\infty}^{\infty} a_l \int_0^{2\pi} d\theta_y e^{il(\theta_x-\theta_y)} e^{lj\theta_y} \\ (H_l^{(1)}(k\rho_x) \int_0^{\rho_x} d\rho_y m_0 \rho_y J_l(k\rho_y) J_j(k\sqrt{n_0}\rho_y) + \\ J_l(k\rho_x) \int_{\rho_x}^R d\rho_y m_0 \rho_y H_l^{(1)}(k\rho_y) J_j(k\sqrt{n_0}\rho_y)) = \\ -u(\underline{x}) + \frac{i\pi}{2} \sum_{l=-\infty}^{\infty} k R D_l a_l J_l(k\sqrt{n_0}\rho_x) e^{il\theta_x}, \|\underline{x}\| < R \end{aligned} \quad (19)$$

where $m_0 = 1 - n_0$ and D_l is defined below Eq. (6). In particular, the second equality can be easily obtained by using the orthogonality of the trigonometric basis and explicit integration formulas for Bessel functions, see (Abramowitz and Stegun, 1965) for details. Now, the first part of (6) can be obtained by substituting in (4) the relations (16), (18) and (19).

When $\|\underline{x}\| > R$, from (16), (17) we obtain the following expression for the integral in (4):

$$\begin{aligned} \frac{ik^2}{4} \int_B H_0^{(1)}(k\|\underline{x}-\underline{y}\|) m(\underline{y}) u(\underline{y}) d\underline{y} = \\ \frac{k}{2\pi} \sum_{l,j=-\infty}^{\infty} \frac{t^l e^{-il\alpha}}{R D_l} \int_0^{2\pi} d\theta_y e^{il(\theta_x-\theta_y)} e^{lj\theta_y} H_l^{(1)}(k\rho_x) \\ \int_0^R d\rho_y m_0 \rho_y J_j(k\rho_y) J_j(k\sqrt{n_0}\rho_y) = \\ t^l \sum_{l=-\infty}^{\infty} \frac{N_l}{D_l} H_l^{(1)}(k\rho_x) e^{il(\theta_x-\alpha)}, \|\underline{x}\| > R \end{aligned} \quad (20)$$

where D_l, N_l are defined below Eq. (6). From (20) the second part of (6) is obtained by using again (4), (16) and (19).